Journal of Solid State Chemistry **160,** 278–286 (2001)
doi:10.1006/jssc.2001.9246, available online at http://www.idealibrary.com on IDEAL®

Two New Organo-Inorganic Hybrid Compounds: Nitrilophosphonates of Aluminum and Copper

Aurelio Cabeza,* Sebastián Bruque,* Antonietta Guagliardi,† and Miguel A.G. Aranda*,[1]

*Departamento de Química Inorgánica, Cristalografía y Mineralogía, Universidad de Málaga, 29071 Málaga, Spain; and †C.N.R.-IRMEC, c/o Dip. Geomineralogico, Campus Universitario, Via Orabona, 4, 70125 Bari, Italy

Received February 12, 2001; in revised form May 2, 2001; accepted May 11, 2001; published online July 3, 2001

Two new organo-inorganic hybrid compounds, aluminum nitrilotris(methylene)trismonohydrogenphosphonate hydrate, $Al[(HO_3PCH_2)_3N]H_2O$, and tricopper(II) bis-nitrilobis(methylene)diphosphonate, $Cu_3[(O_3PCH_2)_2NH_2]_2$, have been synthesized. The crystal structures have been determined *ab initio* from powder diffraction data and refined by the Rietveld method. $Al[(HO_3PCH_2)_3N]H_2O$ is monoclinic, space group $P2_1/n$, with $a = 12.1945(3)$ Å, $b = 9.1129(3)$ Å, $c = 8.5495(2)$ Å, $\beta = 94.317(2)^\circ$, $Z = 4$, and the X-ray powder diffraction pattern has been refined to $R_{wP} = 8.7\%$. $Cu_3[(O_3PCH_2)_2NH_2]_2$ is orthorhombic, space group *Pbca*, with $a = 16.1209(6)$ Å, $b = 9.4890(4)$ Å, $c = 9.4113(4)$ Å, $Z = 4$ and its pattern was refined to $R_{wP} = 13.5\%$. The crystal structure of aluminum phosphonate contains a close packing of inorganic chains, formed by alternating AlO_6 octahedra and O_3PC tetrahedra. These chains are covalently interconnected by the organic groups to give the 3D framework. The structure of copper phosphonate has two distinct copper environments, one a tetragonally elongated tetrahedron and the other a distorted square plane. These structural units are linked by the organic phosphonate. Thermal and infrared data are discussed. © 2001 Academic Press

Key Words: **organo-inorganic composites; *ab initio* structure determination.**

INTRODUCTION

Organo-inorganic hybrid compounds constitute an important field in the area of advanced materials because the structures can be reliably designed in some cases. Metal phosphonate chemistry is one way to synthesize these hybrids and it has attracted a lot of interest in the past two decades (1–3). Metal phosphonates display a wide variety of structures ranging from one-dimensional chains to three-dimensional microporous frameworks, passing thorough the very common layered structures (1). It is possible to have a certain control over the dimensionality of the metal phosphonates by the suitable choice of the phosphonic acid. Furthermore, by carefully choosing anionic ligands forming robust hydrogen bonding networks, one can synthesize hybrid materials with preordained structures that do not depend upon the metal countercation (4, 5).

Functionalized metal phosphonates may have new properties due to the organic functions they include. Consequently, these materials can find a number of practical applications as catalysts, hosts in intercalation compounds, sorbents, ion exchangers, protonic conductors, and components in the preparation of films possessing optical, nonlinear optical, or electronic properties (1, 6). Furthermore, the presence of these functions (such as amines, acids, etc.) in the organic rests opens new possibilities to synthesize tailored materials because of the reactivity of these solids.

We have recently reported the preparation and structures of two divalent lead functionalized triphosphonates, $Pb[(HO_3PCH_2)_3NH]$ and $Pb_2[(O_3PCH_2)_2NH(CH_2PO_3H)]H_2O$ (7), the first alkaline triphosphonate, $Na_2[(HO_3PCH_2)_3NH]1.5H_2O$ (8), and a series of isostructural materials with chemical formula $M[(HO_3PCH_2)_3NH]$ (M^{2+} = Mn, Co, Ni, Zn, Cu, Cd) (5). As part of our research work in phosphonates, in this paper, we described the synthesis and characterization of two new functionalized hybrid materials, $Al[(HO_3PCH_2)_3N]H_2O$ and $Cu_3[(O_3PCH_2)_2NH_2]_2$.

EXPERIMENTAL

Chemicals of reagent quality were obtained from Aldrich and used without further purification. The source of nitrilotris(methylene)triphosphonic (TPA) acid was the 50% w/w commercial solution. NaOH (98%, Prolabo) was used to regulate the pH.

Synthesis of $Al[(HO_3PCH_2)_3N]H_2O$ (AlTP). AlTP was synthesized from a mixture of 0.966 g (12.38 mmol) of $Al(OH)_3$, 57 ml (123.7 mmol) of TPA; and 25 ml of distilled water. This reaction mixture (TPA:Al molar ratio 10:1) is

[1]To whom correspondence should be addressed. Fax.: Int- 34-952132000. E-mail: g_aranda@uma.es.

0022-4596/01 $35.00

a liquid that was loaded in a Teflon-lined autoclave of 250 ml volume. The autoclave vessel was heated at 130°C for 3 days with magnetic stirring. After the thermal treatment, a white powder appeared and the remaining liquid had a pH of 0.2. The solid phase was filtered off, washed with deionized water and with acetone, and dried at 60°C. Analytical data: C, 10.99%; N, 4.16%; H, 3.36%; C/N ratio 3.08. Calculated data for $Al[(HO_3PCH_2)_3N]H_2O$: C, 10.54%; N, 4.11%; H, 3.22%; C/N ratio 3.

Synthesis of $Cu_3[(O_3PCH_2)_2NH_2]_2$ (*CuDP*). CuDP was prepared as a polycrystalline solid by adding 5.105 ml (0.011 mmol) of TPA to 25 ml of 0.665 M $CuCl_2$ in water. No precipitate was formed and the pH was increased to 2 by adding drops of a NaOH solution, 10% w/w. This solution (TPA:Cu molar ratio 2:3) was refluxed for 9 days. An initial green precipitate turned to blue after the first day. The blue solid was filtered off, washed with distilled water, and dried at 60°C. Analytical data: C, 8.01%; N, 4.52%; H, 2.23%; C/N ratio 2.12. Calculated data for $Cu_3[(O_3PCH_2)_2NH_2]_2$: C, 8.07%; N, 4.71%; H, 2.01%; C/N ratio 2.

Techniques. Elemental analysis: Carbon, nitrogen, and hydrogen contents were determined by elemental chemical analysis on a Perkin-Elmer 240 analyzer. *Thermal analysis*: TGA and DTA data were collected on a Rigaku Thermoflex apparatus at the heating rate 10 K min^{-1} in air with calcined Al_2O_3 as internal reference standard in air. *Infrared study*: Infrared spectra were recorded on Perkin Elmer 883 spectrometer in the spectral range 4000–400 cm^{-1}, by using dry KBr pellets containing 2% w/w of the sample. *X-ray powder diffraction.* Room-temperature X-ray powder diffraction patterns were collected on a Philips X'PERT $\Theta/2\Theta$ diffractometer with strictly monochromatic Cu$K\alpha_1$ radiation, 1.540598 Å, by using a Ge (111) primary monochromator. The patterns were recorded between 11 and 70°, in 0.02° steps, counting by 20 s for $Al[(HO_3PCH_2)_3N]H_2O$, and between 6 and 80°, in 0.02° steps, counting by 20 s for $Cu_3[(O_3PCH_2)_2NH_2]_2$.

RESULTS AND DISCUSSION

The structure of AlTP is likely to be protonated as in the case of TPA since it is obtained at low pH and thus can be reported as $Al[(HO_3PCH_2)_2NHCH_2PO_3]H_2O$. The crystal structure as determined supports this description.

In the synthesis of the copper(II) phosphonate, nitrilo*tris*(methylene)*tri*phosphonic acid was also used. However, all synthetic attempts by refluxing or hydrothermal methods (not reported) yielded the same final product which contains copper nitrilo*bis*(methylene)*di*phosphonate. Several syntheses with different TPA:Cu molar ratios were tested and only CuDP was obtained. Under the studied synthetic conditions, a solid with a C/N ratio of 3.0 was never prepared. So, we conclude that an acid solution with Cu^{2+} cations near 100°C catalyzed the rupture of the nitrilotris(methylene)triphosphonic acid to yield nitrilobis(methylene)diphosphonic acid.

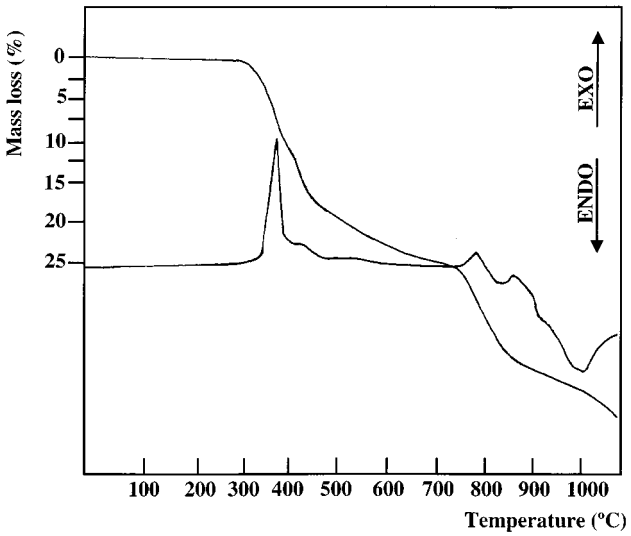

FIG. 1. TGA–DTA curves for $Al[(HO_3PCH_2)_3N]H_2O$.

On the other hand, CuDP could be described as $Cu_3[(O_3PCH_2)_2NH_2]_2$ or alternatively as $Cu_3[O_3PCH_2NHCH_2PO_3H]_2$, as in the aluminum case. However, the IR spectrum and the crystal structure clearly indicate that the nitrogen is linked to two hydrogens. Hence, the chemical formula of CuDP is unambiguously $Cu_3[(O_3PCH_2)_2NH_2]_2$.

Thermal Study

TGA–DTA curves for $Al[(HO_3PCH_2)_3N]H_2O$ are displayed in Fig. 1. DTA shows a strong exotherm centered at 400°C with an associated weight loss of $\sim$ 21% but without a plateau with a constant weight. A second exothermic effect is observed at 820°C followed by a broad endotherm at 1020°C. The first exotherm is due to the combustion of the organic fraction with the releasing of NO_x, CO_2, and H_2O. A thermodiffractometric study indicated that AlTP heated at 500°C is amorphous but at 600°C displays a powder pattern that matches that of $Al(PO_3)_3$ [PDF no. 13-0430] (9). The measured weight loss at 600°C (20.8%) agrees reasonably well with the theoretical value, 22.62%. $Al(PO_3)_3$ decomposes above 700°C to give $AlPO_4$ by releasing out P_2O_5. The exotherm at 820°C and the endotherm at 1020°C are related to this decomposition. AlTP heated at 900°C for 12 h showed the coexistence of $Al(PO_3)_3$ and $AlPO_4$.

TGA–DTA curves for $Cu_3[(O_3PCH_2)_2NH_2]_2$ are displayed in Fig. 2. DTA shows a strong sharp exotherm

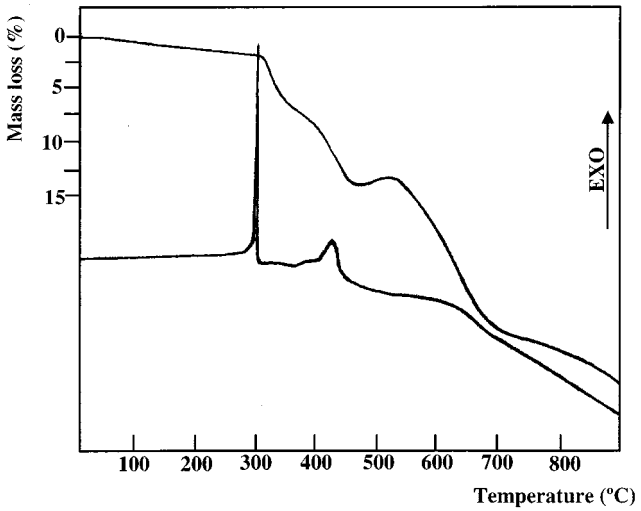

FIG. 2. TGA–DTA curves for $Cu_3[(O_3PCH_2)_2NH_2]_2$.

centered at 320°C and a second broad exotherm at 430°C with an associated weight loss of $\sim 13\%$. The expected weight loss of $Cu_3[(O_3PCH_2)_2NH_2]_2$ to give an amorphous solid of $3CuO \cdot 2P_2O_5$ composition is 12.11%. This loss is due to the combustion of the organic fraction. CuDP undergoes another transformation on heating with an important weight loss which is larger than 25%. The material heated at 900°C for 12 h displays a powder pattern that matches that of $Cu_2P_2O_7$ with PDF no. 71-2177 (10). This second weight loss is due to the release of P_2O_5. The overall expected weight loss of CuDP to give $Cu_2P_2O_7$ is 24.05%, which is slightly lower than the experimental value, 26%. This small disagreement is likely due to the presence of an impurity amorphous phase with a higher organic content which is corroborated by the CNH analysis that gave a measured C/N ratio higher than 2.00.

IR Spectroscopic Study

The IR spectrum for $Al[(HO_3PCH_2)_3N]H_2O$ is shown in Fig. 3a, where the positions of the bands are also given. The region between 4000 and 2000 cm^{-1} shows five bands. The broad absorption at 3330 cm^{-1} is due to the O–H stretching vibration of the hydration water molecule. The position and width suggest that it is interacting strongly through hydrogen bonding. The strong band at 3060 cm^{-1} and the small one at 2800 cm^{-1} are typical of the C–H stretching vibrations of the CH_2 groups. A possible N–H stretching vibration (see discussion below) should be located in this range. The broad bands centered at 2650 and 2370 cm^{-1} are related to PO–H vibrations and are always present in the IR spectra of phosphonates containing hydrogen phosphonate groups (7, 8). The broad band centered at 1610 cm^{-1} is due to the bending vibration of the water

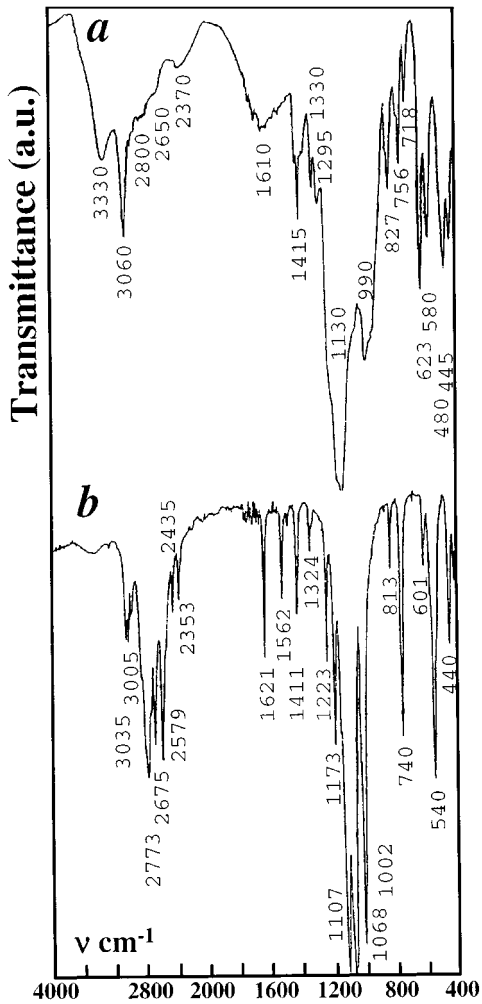

FIG. 3. IR spectra for (a) $Al[(HO_3PCH_2)_3N]H_2O$, and (b) $Cu_3[(O_3PCH_2)_2NH_2]_2$.

molecule. The intense band at 1415 cm^{-1} is typical of the CH_2 deformation vibration and the bands near 1300 cm^{-1} are due to the P–C stretching vibrations of the phosphonates. The two broad and intense bands at 1130 and 990 cm^{-1} are due to the P–O stretching vibrations. The remaining bands are given in Fig. 3a and the assignations are very risky since this complex solid has many vibrations in this region.

The IR spectrum for $Cu_3[(O_3PCH_2)_2NH_2]_2$ is displayed in Fig. 3b together with the position of the bands. There are some similarities between the spectrum of CuDP and that previously discussed for AlTP. However, there are also some differences that must be noted. First, this compound is not hydrated and it does not display the broad bands near 3330 and 1610 cm^{-1} shown by AlTP. Second, this compound has a NH_2 group which results in two sharp bands at 3035 and 3005 cm^{-1} due to the N–H stretching vibrations. Furthermore, the bending NH_2 vibration is now detected

in the IR spectrum as a sharp and intense band at 1562 cm^{-1}. The sharp bands located between 2800 and 2500 cm^{-1} are due to the C–H stretching vibrations. Two small and sharp bands at 2435 and 2353 cm^{-1} are likely overtones and combination bands. It is worth noting that the overall shape of the P–O stretching vibrations is similar to that shown above. However, this compound is more crystalline and the bands are sharper with several vibrations between 1200 and 1000 cm^{-1}. The δCH_2 and ν P–C vibration bands are now located at 1411 and 1324 cm^{-1}, respectively.

Structural Study

The X-ray laboratory powder pattern of $Al[(HO_3PCH_2)_3N]H_2O$ was autoindexed using the TREOR90 program (11), giving a monoclinic unit cell with $a = 12.200(2)$ Å, $b = 9.115(2)$ Å, $c = 8.555(2)$ Å, $\beta = 94.37(1)^\circ$, $V = 948.6$ Å^3, $Z = 4$, V_{at} (non-H atom) $= 13.18$ Å^3/at. $M_{20} = 44$ (12), and $F_{20} = 104$ (0.006, 35) (13). The systematic absences were consistent with $P2_1/n$ space group. The powder pattern of $Cu_3[(O_3PCH_2)_2NH_2]_2$ was also autoindexed using TREOR90, giving an orthorhombic unit cell with $a = 16.085(4)$ Å, $b = 9.475(6)$ Å, $c = 9.414(3)$ Å, $V = 1434.8$ Å^3, $Z = 4$, V_{at} (non-H atom) $= 14.35$ Å^3/at., $M_{20} = 21$, and $F_{20} = 35$ (0.009, 64). The systematic absences indicated *Pbca* as the highest symmetry possible space group.

The crystal structures were solved *ab initio* by powder diffraction data. Both models have been provided by EXPO2000, the new release (in preparation) of the distributed EXPO package (14). In the present version of EXPO2000 the automatic structure solution process includes (1) the pattern decomposition into single integrated intensities by means of the Le Bail algorithm (15); (2) the structure determination by direct methods; (3) a new procedure (still in progress) in which, starting from the E-map, increasing portions of the electron density map are selected and used to phase a progressively extended number of reflections; and (4) a final Fourier-recycling and least-squares refinement procedure (16) to optimize the atomic model. For CuDP, all atoms in the asymmetric unit were supplied by the automatic procedure. At the end of the automatic run for AlTP, all atoms in the asymmetric unit, but one carbon [C(1) in Table 1] and one oxygen (the water molecule oxygen), were correctly located. A Fourier difference map gave the missing carbon.

The structural models obtained in the *ab initio* studies were used as starting models for the Rietveld (17) refinements by using the GSAS package (18). The patterns were fitted by refining initially the overall parameters: background, zero-point error, unit cell, and peak shape values. A pseudo-Voigt peak shape function (19) corrected for asymmetry (20) was used. No preferred orientation effects were observed in both patterns. At this stage, the positions of the atoms were refined using soft constraints for the distances P–O [1.52(1) Å] and P–C [1.80(1) Å] in order to keep a reasonable geometry for the tetrahedral O_3PC groups. Initially, the weight factor for the soft constraints was high, -1000. The weight of the soft constraints was steadily reduced to the final value of -20. The oxygen atom of the water molecule could not be located for AlTP. The final difference Fourier map was featureless. The inclusion of the oxygen in any position which had a small residual electronic density gave unstable refinements with a worst fit. All atoms were refined isotropically for both compounds. The last refinement for AlTP converged to $a = 12.1945(3)$ Å, $b = 9.1129(3)$ Å, $c = 8.5495(2)$ Å, $\beta = 94.317(2)^\circ$, $R_{wP} = 8.7\%$, $R_P = 6.7\%$, and $R_F = 7.5\%$.The last refinement for CuDP converged

TABLE 1
Positional Parameters for $Al[(HO_3PCH_2)_3N]H_2O$

Atom	x	y	z	U_{iso}/Å^2
Al	0.736(1)	0.423(1)	0.233(2)	0.131(5)
P(1)	0.5971(2)	0.171(1)	0.400(1)	0.045(3)
P(2)	0.5740(8)	0.674(1)	0.122(1)	0.068(4)
P(3)	0.7465(8)	0.151(1)	−0.031(1)	0.059(4)
O(1)	0.4765(9)	0.132(2)	0.408(2)	0.055(7)
O(2)	0.609(1)	0.313(1)	0.313(2)	0.081(8)
O(3)	0.641(1)	0.033(1)	0.330(1)	0.056(7)
O(4)	0.621(1)	0.521(1)	0.111(2)	0.082(9)
O(5)	0.543(1)	0.723(2)	−0.046(1)	0.094(8)
O(6)	0.656(1)	0.795(2)	0.165(2)	0.072(8)
O(7)	0.777(1)	0.032(1)	0.088(2)	0.643(8)
O(8)	0.837(1)	0.163(2)	−0.144(2)	0.083(7)
O(9)	0.731(1)	0.298(1)	0.044(2)	0.052(7)
N	0.574(1)	0.162(2)	−0.274(2)	0.040(8)
C(1)	0.659(2)	0.198(2)	0.597(2)	0.05(1)
C(2)	0.542(1)	0.320(1)	−0.245(2)	0.01(1)
C(3)	0.627(1)	0.076(2)	−0.139(3)	0.03(1)

TABLE 2
Bond Lengths (Å) for $Al[(HO_3PCH_2)_3N]H_2O$

Al–O(2)	2.011(14)	Al–O(6)	1.919(14)
Al–O(3)	1.919(14)	Al–O(7)	1.841(14)
Al–O(4)	1.904(14)	Al–O(9)	1.978(14)
P(1)–O(1)	1.519(5)	P(2)–O(4)	1.511(5)
P(1)–O(2)	1.506(5)	P(2)–O(5)	1.522(5)
P(1)–O(3)	1.502(5)	P(2)–O(6)	1.516(5)
P(1)–C(1)	1.806(9)	P(2)–C(2)	1.829(9)
P(3)–O(7)	1.510(5)	N–C(1)	1.61(2)
P(3)–O(8)	1.523(5)	N–C(2)	1.52(2)
P(3)–O(9)	1.502(5)	N–C(3)	1.50(2)
P(3)–C(3)	1.806(9)		

TABLE 3
Positional Parameters for $Cu_3[(O_3PCH_2)_2NH_2]_2$

Atom	x	y	z	$U_{iso}/Å^2$
Cu(1)	$\frac{1}{2}$	0	$\frac{1}{2}$	0.045(3)
Cu(2)	0.6395(3)	0.2447(7)	0.9360(5)	0.062(2)
P(1)	0.5230(6)	0.276(1)	0.687(1)	0.022(3)
P(2)	0.8129(7)	0.055(1)	0.902(1)	0.037(4)
O(1)	0.522(1)	0.118(1)	0.660(2)	0.025(7)
O(2)	0.539(1)	0.311(1)	0.841(1)	0.007(6)
O(3)	0.5798(9)	0.144(2)	0.087(2)	0.014(7)
O(4)	0.6157(8)	− 0.064(2)	0.507(2)	0.034(7)
O(5)	0.7380(9)	0.128(2)	0.966(2)	0.041(9)
O(6)	0.707(1)	0.402(1)	0.870(1)	0.027(8)
N	0.351(1)	0.303(2)	0.743(2)	0.02(1)
C(1)	0.423(2)	0.351(3)	0.650(2)	0.04(1)
C(2)	0.341(2)	0.135(3)	0.768(3)	0.007(10)

TABLE 4
Bond Lengths (Å) for $Cu_3[(O_3PCH_2)_2NH_2]_2$

Cu(1)–O(1)	1.907(14)	Cu(2)–O(2)	1.958(14)
Cu(1)–O(1)	1.907(14)	Cu(2)–O(3)	1.964(14)
Cu(1)–O(2)	2.418(12)	Cu(2)–O(5)	1.959(14)
Cu(1)–O(2)	2.418(12)	Cu(2)–O(6)	1.954(16)
Cu(1)–O(4)	1.962(14)		
Cu(1)–O(4)	1.962(14)		
P(1)–O(1)	1.522(2)	P(2)–O(4)	1.518(2)
P(1)–O(2)	1.512(2)	P(2)–O(5)	1.511(2)
P(1)–O(3)	1.516(2)	P(2)–O(6)	1.522(2)
P(1)–C(1)	1.80(3)	P(2)–C(2)	1.83(2)
N–C(1)	1.520(3)	N–C(2)	1.614(3)

to $a = 16.1209(6)$ Å, $b = 9.4890(4)$ Å, $c = 9.4113(4)$ Å, $R_{wP} = 13.5\%$, $R_P = 10.2\%$, and $R_F = 6.1\%$. Final positionaland thermal parameters for AlTP are presented in Table 1 and bond lengths in Table 2. Final positional and thermal parameters for CuDP are given in Table 3 and bond lengths in Table 4. The final Rietveld plots for AlTP and CuDP are given in Figs. 4 and 5, respectively.

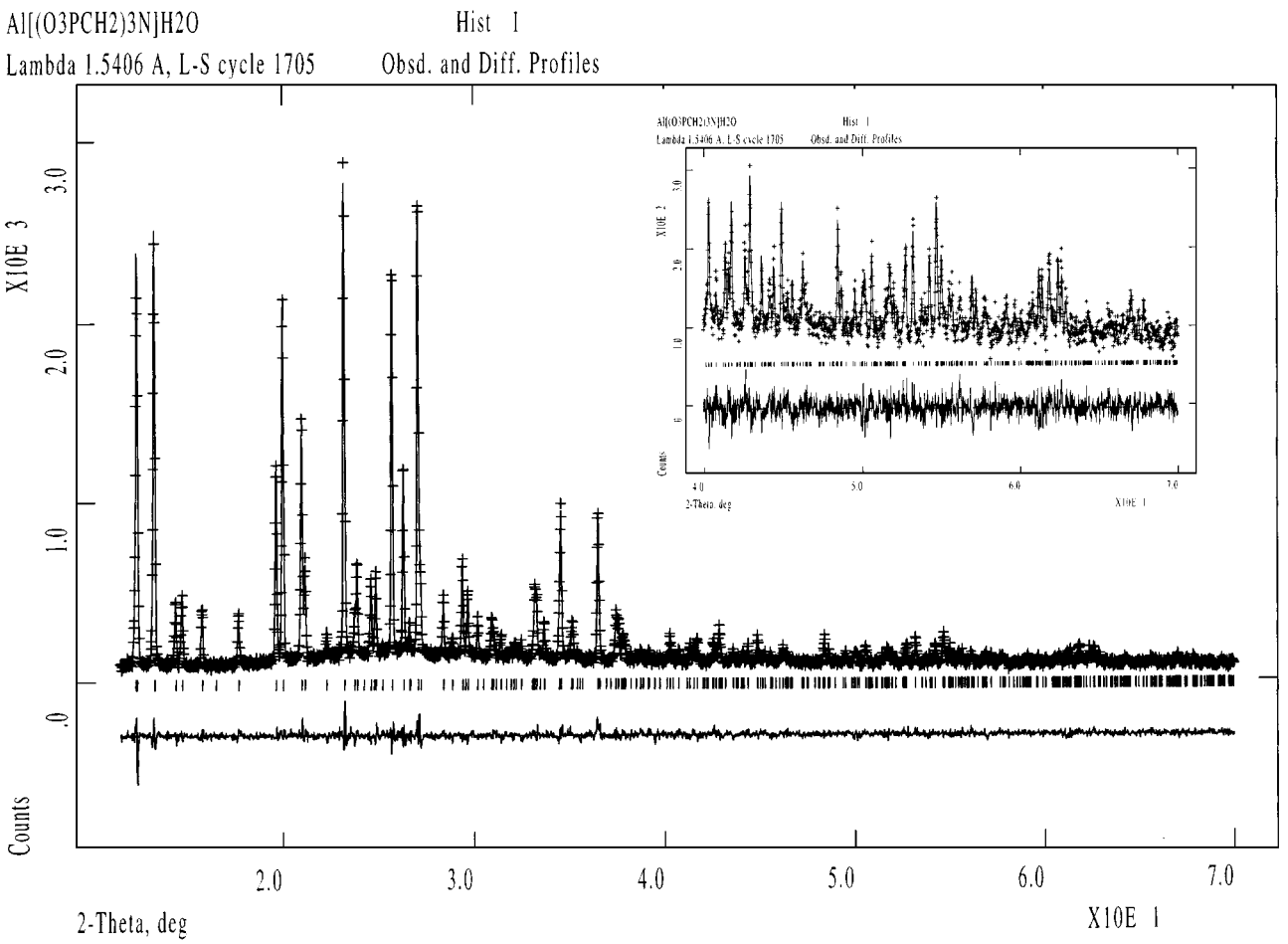

FIG. 4. X-ray powder diffraction Rietveld plot for $Al[(HO_3PCH_2)_3N]H_2O$.

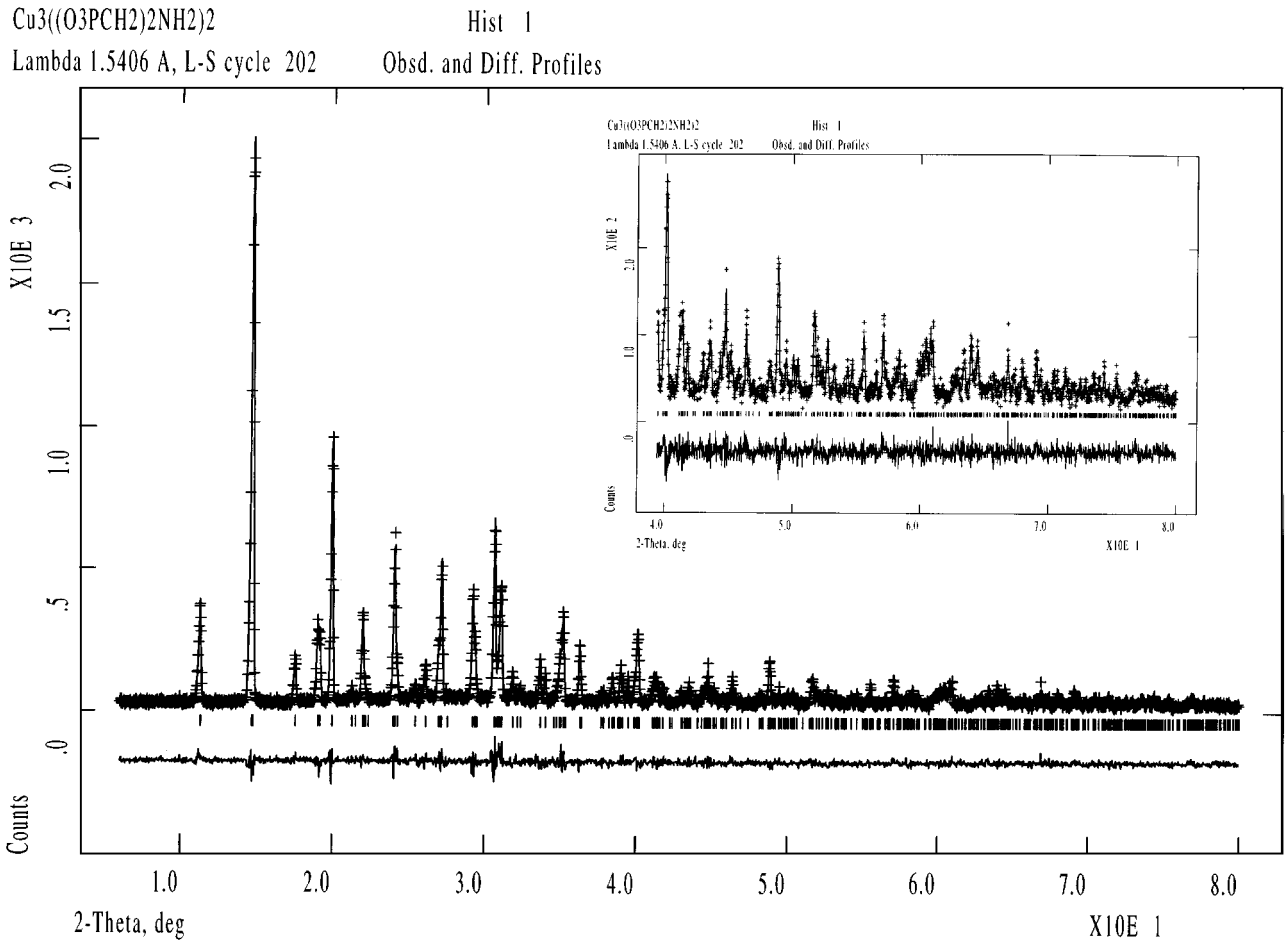

FIG. 5. X-ray powder diffraction Rietveld plot for $Cu_3[(O_3PCH_2)_2NH_2]_2$.

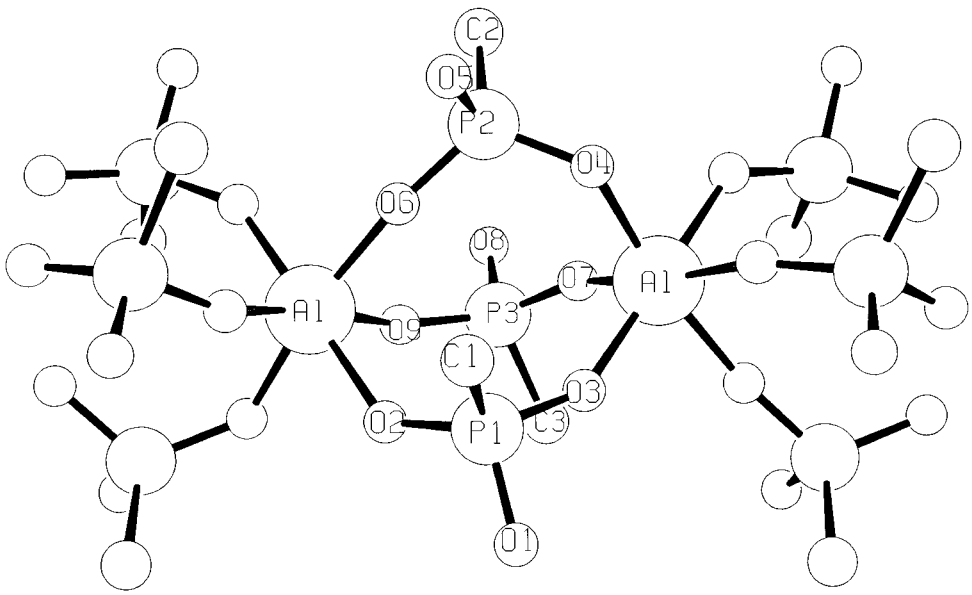

FIG. 6. Ball and stick view of the inorganic chains of $Al[(HO_3PCH_2)_3N]H_2O$ running along the *b*-axis. AlO_6 octahedra and PO_3C tetrahedra are shown with the atoms labeled. Nitrogen atoms are not shown for clarity and the oxygen of the water molecule and the hydrogens were not located.

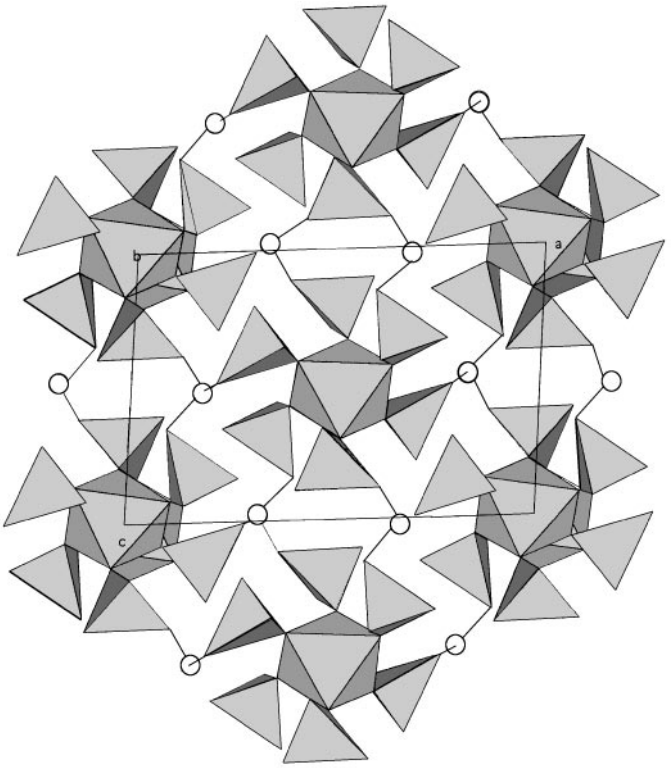

FIG. 7. [010] polyhedral view of the crystal structure of $Al[(HO_3PCH_2)_3N]H_2O$ with the nitrogen atoms shown as balls.

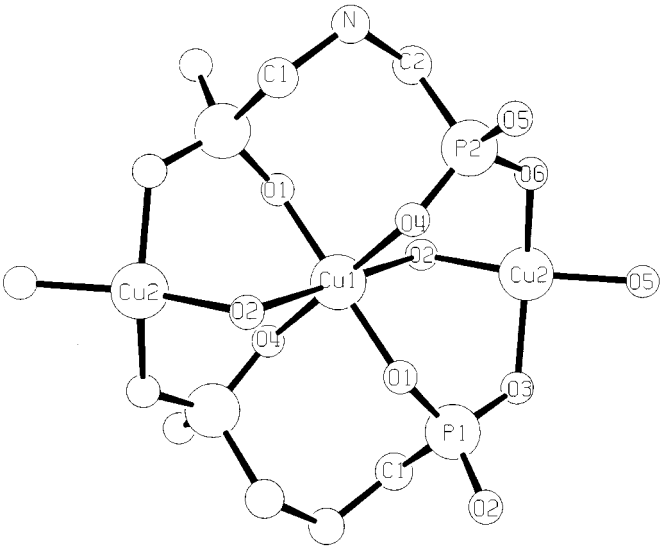

FIG. 8. Ball and stick view of a fraction the crystal structure of $Cu_3[(O_3PCH_2)_2NH_2]_2$ with the atoms labeled. $Cu(1)O_6$ distorted octahedron and $Cu(2)O_4$ distorted square plane and PO_3C tetrahedra are shown.

The crystal structure of AlTP is three-dimensional with chains formed by AlO_6 octahedra and O_3PC tetrahedra running along the [010] direction (Fig. 6). The AlO_6 octahedra are linked along the chains by the phosphonate groups. The AlO_6 distorted octahedron has an average Al–O distance of 1.929 Å which compares well with the expected value, 1.935 Å, from the Shannon ionic radii (21). The polyhedral linkage along the chains resembles the "lantern unit" of NASICON phosphates but totally condensed (22, 23). Only two oxygens of the phosphonate tetrahedra, O_3PC, participate in the linkage of the chains and the remaining oxygen and carbon atoms point out (Figs. 6 and 7). Oxygens O(1), O(5), and O(8) are not bonded to the aluminum and so, they are the POH groups. These "cylindrical" chains $[\ldots{-}O_3{-}Al{-}O_3{-}3P\ldots]$ are close packed (Fig. 7) in the *ac* plane. The linear inorganic chains are not isolated but they are covalently branched through the organic part, formed by the methylene and nitrogen groups $3P \equiv (CH_2)_3N$, giving the 3D network. There is a short contact between O(1) and N of 2.73 Å. So, the nitrogen atom could be protonated, R_3NH^+, and the phosphonate P(1) group should be negatively charged. It may be mentioned that the oxygen atom of the water molecule in this structure could not be located by the difference Fourier approach because the water molecule might be disordered in the interchain space.

The crystal structure of CuDP is also three-dimensional with two environments for the copper atoms. Cu(1) is in a tetragonally elongated oxygen octahedron with three pairs of Cu–O distances, 1.91, 1.96, and 2.42 Å. The oxygen environment for Cu(2) is a distorted square plane with four similar Cu–O distances of about 1.96 Å (see Fig. 8). These oxygen environments agree with the Jahn–Teller effect shown by the Cu^{2+} cations. The multiplicity of the $Cu(1)O_6$ octahedron is half that of the $Cu(2)O_4$ square planes. The crystal structure can be described by layers of CuO_6 octahedra and phosphonate tetrahedra packed along the *a*-axis. These layers are covalently bonded to each other by the CuO_4 square planes, and the organic $= (CH_2)_2NH_2$ groups (Fig. 9). This 3D structure encloses small channels running along the *b*-axis, where the hydrogens of the NH_2 groups are located. In this structure, all oxygens of the phosphonate groups are strongly bonded to the coppers. So, the proton must be linked to the nitrogen, ruling out the possible existence of a hydrogen phosphonate, O_2POH, group. If we take into account the van der Waals radii, the channels are very small and this solid cannot be used as a molecular sieve. This copper phosphonate is not expected to have magnetic properties as the copper oxygen polyhedra are isolated with a unique link between the CuO_6 and CuO_4 groups mediated by O(2) which is long bonded to the octahedron because of the Jahn–Teller effect. There is not an infinite Cu–O–Cu linking in the structure.

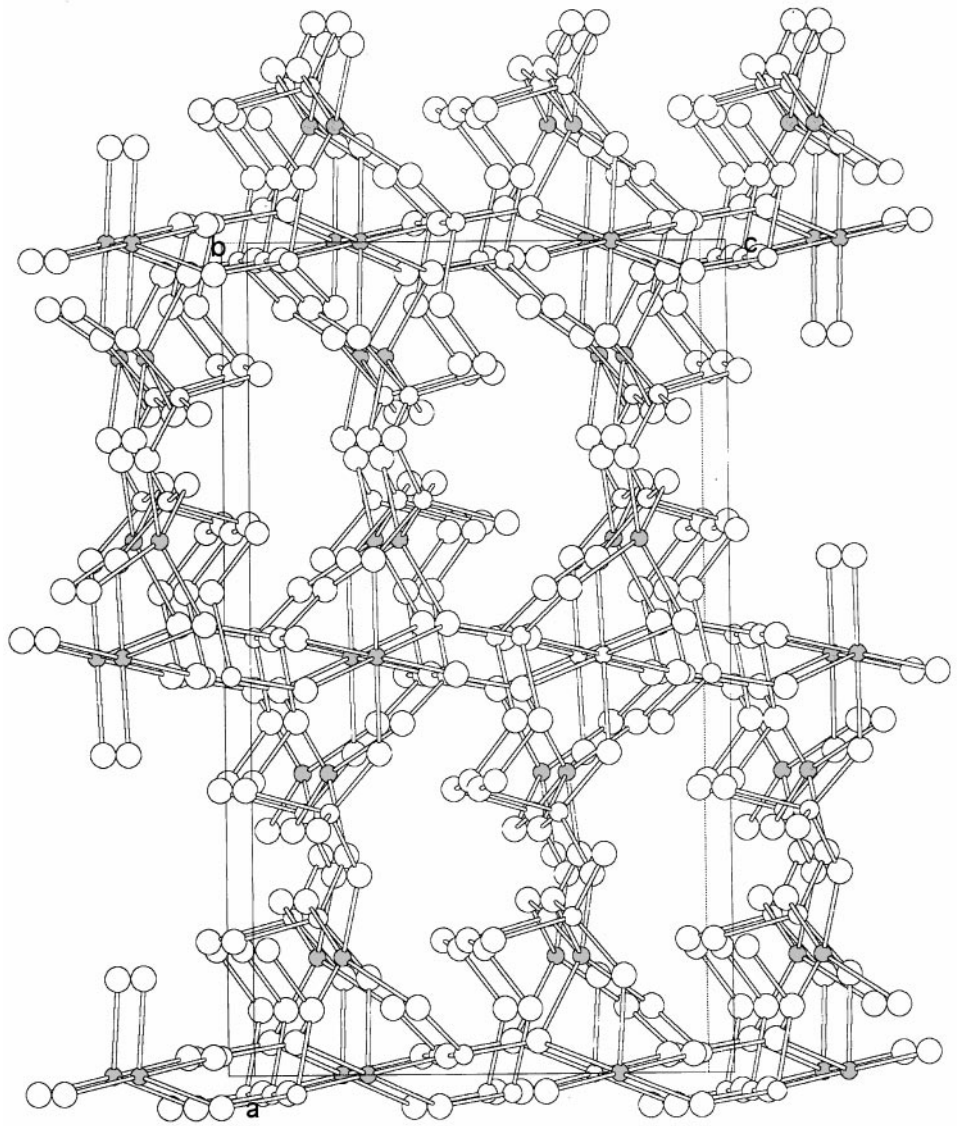

FIG. 9. [010] ball and stick view of the crystal structure of $Cu_3[(O_3PCH_2)_2NH_2]_2$.

ACKNOWLEDGMENTS

The work in Málaga was supported by research grant FQM-113 (of Junta de Andalucía).

REFERENCES

1. A. Clearfield, "Progress in Inorganic Chemistry" (K. D. Karlin, Ed.), Vol. 47, p. 371, Wiley, New York, 1998.
2. S. Drumel, V. Penicaud, D. Deniaud, and B. Bujoli, *Trends Inorg. Chem.* **4,** 13 (1996).
3. M. E. Thompson, *Chem. Mater.* **6,** 1168 (1994).
4. C. V. K. Sharma and A. Clearfield, *J. Am. Chem. Soc.* **122,** 1558 (2000); C. V. K. Sharma and A. Clearfield, *J. Am. Chem. Soc.* **122,** 4394 (2000).
5. C. V. K. Sharma, A. Clearfield, A. Cabeza, M. A. G. Aranda, and S. Bruque, *J. Am. Chem. Soc.* **123,** 2885 (2001).
6. R. LaDuca, D. Rose, J. R. D. DeBord, R. C. Haushalter, C. J. O'Connor, and J. Zubieta, *J. Solid State Chem.* **123,** 408 (1996).
7. A. Cabeza, M. A. G. Aranda, and S. Bruque, *J. Mater. Chem.* **9,** 571 (1999).
8. H. S. Martínez-Tapia, A. Cabeza, S. Bruque, P. Pertierra, S. García-Granda, and M. A. G. Aranda, *J. Solid State Chem.* **151,** 122 (2000).
9. U.S. Natl. Bur. Stand. Monogr. **25,** 2 (1963).
10. B. E. Robertson and V. Calvo, *Acta Crystallogr.* **22,** 665 (1967).
11. P. E. Werner, L. Eriksson, and M. Westdahl, *J. Appl. Crystallogr.* **18,** 367 (1985).
12. P. M. Wolff, *J. Appl. Crystallogr.* **1,** 108 (1968).
13. G. S. Smith and R. L. Snyder, *J. Appl. Crystallogr.* **12,** 60 (1979).
14. A. Altomare, M. C. Burla, M. Camalli, B. Carrozzini, G. L. Cascarano, C. Giacovazzo, A. Guagliardi, A. G. G. Moliterni, G. Polidori, and R. Rizzi, *J. Appl. Crystallogr.* **32,** 339 (1999).
15. A. Le Bail, H. Duroy, and J. L. Fourquet, *Mater. Res. Bull.* **23,** 447 (1988).

16. A. Altomare, G. L. Cascarano, C. Giacovazzo, A. Guagliardi, M. C. Burla, G. Polidori, and M. Camalli, *J. Appl. Crystallogr.* **27,** 435 (1994).
17. H. M. Rietveld, *J. Appl. Crystallogr.* **2,** 65 (1969).
18. A. C. Larson and R. B. von Dreele, Los Alamos National Lab. Rep. No. LA-UR-86-748, LANL, Los Alames, NM, 1994.
19. P. Thompson, D. E. Cox, and J. B. Hasting, *J. Appl. Crystallogr.* **20,** 79 (1987).
20. L. W. Finger, D. E. Cox, and A. P. Jephcoat, *J. Appl. Crystallogr.* **27,** 892 (1994); M. A. G. Aranda, E. R. Losilla, A. Cabeza, and S. Bruque, *J. Appl. Crystallogr.* **31,** 16 (1998).
21. R. D. Shannon, *Acta Crystallogr. A* **32,** 751 (1976).
22. H. Y. P. Hong, *Mater. Res. Bull.* **11,** 173 (1976).
23. E. R. Losilla, M. A. G. Aranda, S. Bruque, M. A. París, J. Sanz, and A. R. West, Chem. Mater. **10,** 665 (1998).